AIP | The Journal of Chemical Physics

Relations between Rydberg-valence interactions in the O 2 molecule

B. R. Lewis, S. T. Gibson, S. S. Banerjee, and H. Lefebvre-Brion

Citation: The Journal of Chemical Physics **113**, 2214 (2000); doi: 10.1063/1.482035
View online: http://dx.doi.org/10.1063/1.482035
View Table of Contents: http://scitation.aip.org/content/aip/journal/jcp/113/6?ver=pdfcov
Published by the AIP Publishing

Articles you may be interested in

Extensive ab initio study of the valence and low-lying Rydberg states of BBr including spin-orbit coupling
J. Chem. Phys. **124**, 194307 (2006); 10.1063/1.2197830

Rydberg-valence interactions of CO, and spectroscopic evidence characterizing the C ′ 1 Σ + valence state
J. Chem. Phys. **121**, 292 (2004); 10.1063/1.1756579

Spectroscopic characterization of the metastable 3pπ 3 Π 0 + ,0 − valence states and the 4s 3 Σ + Rydberg states of the MgKr and MgXe van der Waals molecules
J. Chem. Phys. **107**, 10492 (1997); 10.1063/1.474213

Two-dimensional photoelectron spectroscopy of acetylene: Rydberg-valence interaction between the (3σ g) −1 (3pσ u) 1 and (3σ g) −1 (3σ u) 1 states
J. Chem. Phys. **106**, 4902 (1997); 10.1063/1.473991

Ab initio configuration interaction calculations of the predissociation of rovibrational levels of the C 3 Π g and d 1 Π g 3sσ Rydberg states of the oxygen molecule
J. Chem. Phys. **106**, 1123 (1997); 10.1063/1.473208

How can you **REACH 100%** of researchers at the Top 100 Physical Sciences Universities? (TIMES HIGHER EDUCATION RANKINGS, 2014)

With *The Journal of Chemical Physics*.

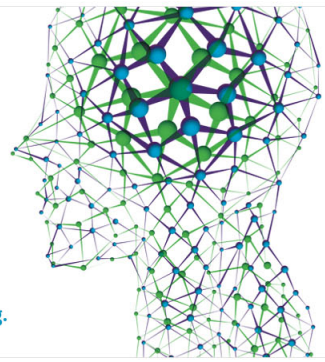

AIP | The Journal of Chemical Physics

THERE'S POWER IN NUMBERS. Reach the world with AIP Publishing.

This article is copyrighted as indicated in the article. Reuse of AIP content is subject to the terms at: http://scitation.aip.org/termsconditions. Downloaded to IP: 150.203.176.45 On: Fri, 24 Apr 2015 03:26:09

Relations between Rydberg-valence interactions in the O_2 molecule

B. R. Lewis, S. T. Gibson, and S. S. Banerjee
Research School of Physical Sciences and Engineering, The Australian National University, Canberra, ACT 0200, Australia

H. Lefebvre-Brion
Laboratoire de Photophysique Moléculaire, Bâtiment 213, Université de Paris-Sud, 91405 Orsay Cedex, France

(Received 7 March 2000; accepted 12 May 2000)

Using a single-configuration formulation, analytical expressions are derived for the $(X\,^2\Pi_g)\,ns\sigma_g$, $np\pi_u$, and $np\sigma_u$ Rydberg-valence interaction matrix elements in O_2. In addition, new results from diabatic, coupled-channel deperturbations of experimental data dependent on these interactions are reported for $n=3$ and 4. Using these results, the large differences in magnitude between the Rydberg-valence couplings for the constituent states of the $np\pi_u$ Rydberg complex that are predicted by the analytical expressions are verified experimentally. Effective values for several two-electron integrals are obtained semiempirically through comparison between analytical expressions and deperturbed experimental values for the Rydberg-state energies and Rydberg-valence couplings, allowing predictions to be made for the spectroscopy of the $np\pi_u\,^1\Sigma_u^-$ Rydberg states which have yet to be observed. © *2000 American Institute of Physics.* [S0021-9606(00)31530-6]

I. INTRODUCTION

Interactions between isosymmetric Rydberg and valence molecular electronic states occurring in the same energy region are responsible for a wide range of interesting spectral phenomena, including perturbations, predissociations, lineshape asymmetries, and intensity quantum-interference effects. The magnitudes of such Rydberg-valence interactions vary from small, where a *diabatic* picture is appropriate, through intermediate, to large, where an *adiabatic* picture applies and strongly avoided crossings occur between the pure Rydberg and valence states.

O_2 is one of the few molecules for which Rydberg-valence interactions have been extensively studied, both theoretically and experimentally. However, there have been no comprehensive studies of the relations between the interactions involving states of different symmetries associated with the various series of $nl\lambda$ Rydberg complexes converging on the $X\,^2\Pi_g$ state of O_2^+. *Ab initio* studies of the Rydberg-valence interactions in O_2 have been performed for the $3s\sigma_g$ and $4s\sigma_g\,^1\Pi_g$;[1] $3s\sigma_g$ and $4s\sigma_g\,^3\Pi_g$;[1,2] $3p\sigma_u$ and $4p\sigma_u\,^1\Pi_u$;[3] $3p\sigma_u$ and $4p\sigma_u\,^3\Pi_u$;[3,4] $3p\pi_u$ to $6p\pi_u\,^3\Sigma_u^-$;[4–8] $3p\pi_u$, $4p\pi_u$, $6p\pi_u$ and $7p\pi_u\,^1\Sigma_u^+$;[5,6,9] $3p\pi_u$ to $7p\pi_u\,^1\Delta_u$;[3,5,6] and $3p\pi_u\,^3\Delta_u$ states.[4] In addition, analyses of experimental spectra using effective-parameter, diabatic-basis theoretical treatments of the Rydberg-valence interactions have yielded semiempirical estimates of the interaction matrix elements for the $3s\sigma_g$ and $4s\sigma_g\,^1\Pi_g$,[10,11] $3s\sigma_g$ and $4s\sigma_g\,^3\Pi_g$,[11–14] $3p\pi_u\,^3\Sigma_u^-$,[15–17] and $3p\sigma_u$ to $6p\sigma_u\,^3\Pi_u$ states.[18] These estimates have resulted from the use of both perturbative[10,12,14] and coupled-channel[11,13,15–18] methods.

Two types of Rydberg-valence mixing can be described in terms of the single-configuration approximation.[19] First, in case (1), the configurations of the Rydberg and valence states differ by two orbitals. This is the case in O_2 for valence states of the $\cdots(1\pi_u)^3(1\pi_g)^3$ molecular-orbital configuration[20] and Rydberg states of the $\cdots(1\pi_u)^4(1\pi_g)(np\pi_u)$ configuration, shown schematically in a diabatic representation in Fig. 1(a), and also for the $\cdots(3\sigma_g)(1\pi_u)^4(1\pi_g)^3$ valence and $\cdots(3\sigma_g)^2(1\pi_u)^4(1\pi_g)(ns\sigma_g)$ Rydberg states, shown in Fig. 1(b). Second, in case (2), the configurations of the Rydberg and valence states differ by only one orbital. This is the case in O_2 for the $\cdots(1\pi_u)^4(1\pi_g)(np\sigma_u)$ Rydberg and $\cdots(1\pi_u)^4(1\pi_g)(3\sigma_u)$ valence states, shown in Fig. 1(c), which differ only in the last orbital.

In this work, we present analytical expressions for the $ns\sigma_g$, $np\pi_u$, and $np\sigma_u$ Rydberg-valence interaction matrix elements in O_2, based on a single-configuration formulation. New results from semiempirical, coupled-channel analyses of experimental spectra are also presented and compared with these expressions, other semiempirical data, and *ab initio* calculations. Finally, predictions are made for the spectroscopy of the $np\pi_u\,^1\Sigma_u^-$ Rydberg states which have yet to be observed.

II. THE SINGLE-CONFIGURATION APPROXIMATION

A. Rydberg energies

The single-configuration approximation has often been applied to the calculation of Rydberg states, in particular using the method pioneered by Lefebvre-Brion and Moser[21] (see also Ref. 22) and later used by Hunt and Goddard[23] under the improved virtual orbital (IVO) name. If the Rydberg states arising from the $\pi_g\,np\pi_u$ configuration are represented in the single-configuration approximation and if the

 © 2000 American Institute of Physics

This article is copyrighted as indicated in the article. Reuse of AIP content is subject to the terms at: http://scitation.aip.org/termsconditions. Downloaded to IP: 150.203.176.45 On: Fri, 24 Apr 2015 03:26:09

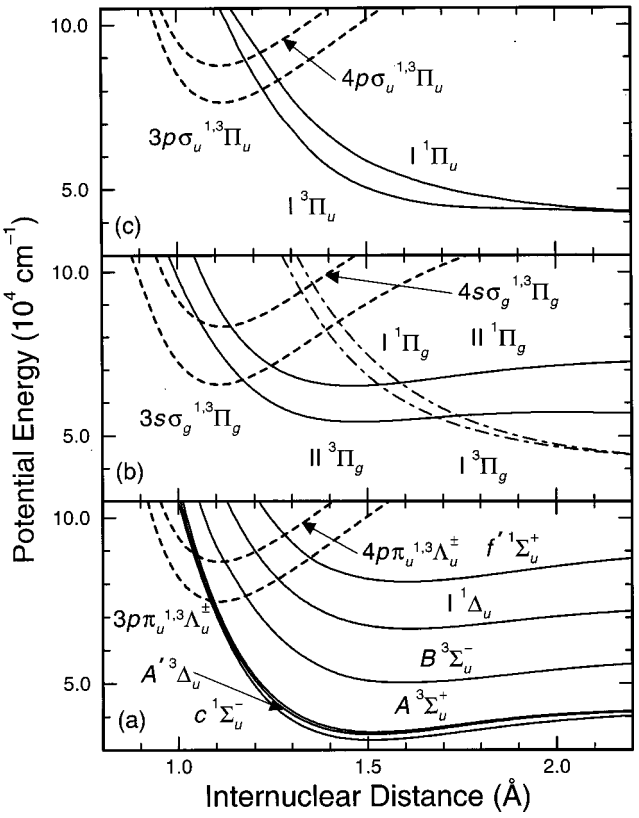

FIG. 1. Schematic diabatic potential-energy curves for the lower members of the *ns* and *np* Rydberg series converging on the $X\,{}^2\Pi_g$ state of O_2^+ (dashed lines), together with those for the interacting valence states (solid lines). The energy scale is referenced to the minimum in the $X\,{}^3\Sigma_g^-$ potential-energy curve (not shown) and the closely spaced constituent states of each Rydberg complex are represented by a single curve. (a) The $\cdots(1\pi_u)^3(1\pi_g)^3\,{}^{1,3}\Lambda_u^{\pm}$ valence and $\cdots(1\pi_u)^4(1\pi_g)(np\pi_u)\,{}^{1,3}\Lambda_u^{\pm}$ Rydberg states for $n=3$ and 4 ($^{1,3}\Lambda_u^{\pm}={}^{1,3}\Sigma_u^{\pm}$, $^{1,3}\Delta_u$). (b) The $\cdots(3\sigma_g)\times(1\pi_u)^4(1\pi_g)^3\,{}^{1,3}\Pi_g$ valence and $\cdots(3\sigma_g)^2(1\pi_u)^4(1\pi_g)(ns\sigma_g)\,{}^{1,3}\Pi_g$ Rydberg states for $n=3$ and 4. The $\cdots(3\sigma_g)^2(1\pi_u)^3(1\pi_g)^2(3\sigma_u)\,{}^{1,3}\Pi_g$ valence states are also indicated (dotted–dashed lines). (c) The $\cdots(1\pi_g)\times(3\sigma_u)\,{}^{1,3}\Pi_u$ valence and $\cdots(1\pi_g)(np\sigma_u)\,{}^{1,3}\Pi_u$ Rydberg states for $n=3$ and 4.

same orbitals are used for each of the states, the relative energies of these states are given by the Recknagel expressions:[24]

$$E(^1\Sigma_u^-)=E-J^{(2)}+K^{(2)}, \tag{1a}$$

$$E(^3\Delta_u)=E, \tag{1b}$$

$$E(^3\Sigma_u^+)=E+J^{(2)}-K^{(2)}, \tag{1c}$$

$$E(^3\Sigma_u^-)=E+2K^{(0)}-J^{(2)}-K^{(2)}, \tag{1d}$$

$$E(^1\Delta_u)=E+2K^{(0)}, \tag{1e}$$

$$E(^1\Sigma_u^+)=E+2K^{(0)}+J^{(2)}+K^{(2)}, \tag{1f}$$

where the exchange (K) and direct (J) integrals are given by

$$K^{(0)}=\int \pi_g^{+*}(1)np\pi_u^+(1)\frac{e^2}{r_{12}}np\pi_u^{-*}(2)\pi_g^-(2)d\tau_1\,d\tau_2, \tag{2a}$$

$$K^{(2)}=\int \pi_g^{+*}(1)np\pi_u^-(1)\frac{e^2}{r_{12}}np\pi_u^{-*}(2)\pi_g^+(2)d\tau_1\,d\tau_2, \tag{2b}$$

$$J^{(2)}=\int \pi_g^{+*}(1)\pi_g^-(1)\frac{e^2}{r_{12}}np\pi_u^{-*}(2)np\pi_u^+(2)d\tau_1\,d\tau_2. \tag{2c}$$

The magnitudes of these integrals depend on the atomic basis set used in the self-consistent calculations, but they are expected to be in the order $K^{(0)}>J^{(2)}>K^{(2)}$.

Diabatic observed values, i.e., deperturbed experimental values for the energies of the Rydberg states, can be fitted to the Recknagel expressions [Eq. (1)] and effective values for the integrals obtained. If one of the states has not been observed, knowledge of these integrals derived from the energies of the other states allows a value for its energy to be predicted semiempirically.

For the other Rydberg states treated in this paper, i.e., the $^{1,3}\Pi$ states arising from the $\pi_g ns\sigma_g$ and $\pi_g np\sigma_u$ configurations, the single-configuration approximation leads to the well-known expression

$$E(^3\Pi)=E(^1\Pi)-2K^{(0)}_{\pi_g,n\sigma}. \tag{3}$$

B. Rydberg-valence interactions

Using the single-configuration approximation for both the Rydberg and valence states, analytical expressions for the Rydberg-valence couplings can be obtained from the wave functions given in Table I in the form of the diagonals of the relevant determinants.

The electrostatic interactions between valence and Rydberg states of the same symmetry with the configurations $\cdots(1\pi_u)^3(1\pi_g)^3$ and $\cdots(1\pi_u)^4(1\pi_g)(np\pi_u)$, respectively, wave functions for which are given in the first part of Table I, can be expressed in terms of the two-electron integrals

$$M^{(0)}=\int \pi_u^{+*}(1)\pi_g^+(1)\frac{e^2}{r_{12}}np\pi_u^{-*}(2)\pi_g^-(2)d\tau_1\,d\tau_2, \tag{4a}$$

$$M^{(2)}=\int \pi_u^{+*}(1)\pi_g^-(1)\frac{e^2}{r_{12}}np\pi_u^{-*}(2)\pi_g^+(2)d\tau_1\,d\tau_2. \tag{4b}$$

These integrals have the same sign and $|M^{(0)}|>|M^{(2)}|$. Resulting expressions for the Rydberg-valence coupling matrix elements $H^{\rm el}(^{1,3}\Lambda_u^{\pm})=\langle \pi_u^3\pi_g^3\,{}^{1,3}\Lambda_u^{\pm}|\mathbf{H}^{\rm el}|\pi_g np\pi_u\,{}^{1,3}\Lambda_u^{\pm}\rangle$ are

$$H^{\rm el}(^1\Sigma_u^-)=-2M^{(2)}=2H^{\rm el}(^3\Delta_u), \tag{5a}$$

$$H^{\rm el}(^3\Sigma_u^+)=0, \tag{5b}$$

$$H^{\rm el}(^3\Sigma_u^-)=2M^{(0)}, \tag{5c}$$

$$H^{\rm el}(^1\Delta_u)=2M^{(0)}-M^{(2)}, \tag{5d}$$

$$H^{\rm el}(^1\Sigma_u^+)=-2M^{(0)}+2M^{(2)}. \tag{5e}$$

As in the case of the two-electron integrals involved in the Recknagel energy expressions of Sec. II A, effective values for $|M^{(0)}|$ and $|M^{(2)}|$ can be obtained semiempirically through a comparison between the Rydberg-valence cou-

This article is copyrighted as indicated in the article. Reuse of AIP content is subject to the terms at: http://scitation.aip.org/termsconditions. Downloaded to IP: 150.203.176.45 On: Fri, 24 Apr 2015 03:26:09

TABLE I. Electronic wave functions for interacting valence and Rydberg states of O_2 ($\Sigma=0$).[a]

Symmetry	Character	Ω	Wave function
$^3\Sigma_u^-$	Valence	0	$\frac{1}{2}\{\lvert\pi_u^+\alpha\,\pi_u^+\beta\,\pi_g^-\alpha\,\pi_g^-\beta[\pi_u^-\pi_g^+(\alpha\beta+\beta\alpha)]\rvert$ $-\lvert\pi_u^-\alpha\,\pi_u^-\beta\,\pi_g^+\alpha\,\pi_g^+\beta[\pi_u^+\pi_g^-(\alpha\beta+\beta\alpha)]\rvert\}$
	Rydberg	0	$\frac{1}{2}\{\lvert\pi_u^+\alpha\,\pi_u^+\beta\,\pi_u^-\alpha\,\pi_u^-\beta[\pi_g^+np\pi_u^-(\alpha\beta+\beta\alpha)]\rvert$ $-\lvert\pi_u^+\alpha\,\pi_u^+\beta\,\pi_u^-\alpha\,\pi_u^-\beta[\pi_g^-np\pi_u^+(\alpha\beta+\beta\alpha)]\rvert\}$
$^1\Sigma_u^+$	Valence	0	$\frac{1}{2}\{\lvert\pi_u^+\alpha\,\pi_u^+\beta\,\pi_g^-\alpha\,\pi_g^-\beta[\pi_u^-\pi_g^+(\alpha\beta-\beta\alpha)]\rvert$ $+\lvert\pi_u^-\alpha\,\pi_u^-\beta\,\pi_g^+\alpha\,\pi_g^+\beta[\pi_u^+\pi_g^-(\alpha\beta-\beta\alpha)]\rvert\}$
	Rydberg	0	$\frac{1}{2}\{\lvert\pi_u^+\alpha\,\pi_u^+\beta\,\pi_u^-\alpha\,\pi_u^-\beta[\pi_g^+np\pi_u^-(\alpha\beta-\beta\alpha)]\rvert$ $+\lvert\pi_u^+\alpha\,\pi_u^+\beta\,\pi_u^-\alpha\,\pi_u^-\beta[\pi_g^-np\pi_u^+(\alpha\beta-\beta\alpha)]\rvert\}$
$^3\Sigma_u^+$	Valence	0	$\frac{1}{2}\{\lvert\pi_u^+\alpha\,\pi_u^+\beta\,\pi_g^-\alpha\,\pi_g^-\beta[\pi_u^-\pi_g^+(\alpha\beta+\beta\alpha)]\rvert$ $+\lvert\pi_u^-\alpha\,\pi_u^-\beta\,\pi_g^+\alpha\,\pi_g^+\beta[\pi_u^+\pi_g^-(\alpha\beta+\beta\alpha)]\rvert\}$
	Rydberg	0	$\frac{1}{2}\{\lvert\pi_u^+\alpha\,\pi_u^+\beta\,\pi_u^-\alpha\,\pi_u^-\beta[\pi_g^+np\pi_u^-(\alpha\beta+\beta\alpha)]\rvert$ $+\lvert\pi_u^+\alpha\,\pi_u^+\beta\,\pi_u^-\alpha\,\pi_u^-\beta[\pi_g^-np\pi_u^+(\alpha\beta+\beta\alpha)]\rvert\}$
$^1\Sigma_u^-$	Valence	0	$\frac{1}{2}\{\lvert\pi_u^+\alpha\,\pi_u^+\beta\,\pi_g^-\alpha\,\pi_g^-\beta[\pi_u^-\pi_g^+(\alpha\beta-\beta\alpha)]\rvert$ $-\lvert\pi_u^-\alpha\,\pi_u^-\beta\,\pi_g^+\alpha\,\pi_g^+\beta[\pi_u^+\pi_g^-(\alpha\beta-\beta\alpha)]\rvert\}$
	Rydberg	0	$\frac{1}{2}\{\lvert\pi_u^+\alpha\,\pi_u^+\beta\,\pi_u^-\alpha\,\pi_u^-\beta[\pi_g^+np\pi_u^-(\alpha\beta-\beta\alpha)]\rvert$ $-\lvert\pi_u^+\alpha\,\pi_u^+\beta\,\pi_u^-\alpha\,\pi_u^-\beta[\pi_g^-np\pi_u^+(\alpha\beta-\beta\alpha)]\rvert\}$
$^3\Delta_u$	Valence	2	$\frac{1}{\sqrt{2}}\lvert\pi_u^+\alpha\,\pi_u^+\beta\,\pi_g^+\alpha\,\pi_g^+\beta[\pi_u^-\pi_g^-(\alpha\beta+\beta\alpha)]\rvert$
	Rydberg	2	$\frac{1}{\sqrt{2}}\lvert\pi_u^+\alpha\,\pi_u^+\beta\,\pi_u^-\alpha\,\pi_u^-\beta[\pi_g^+np\pi_u^+(\alpha\beta+\beta\alpha)]\rvert$
$^1\Delta_u$	Valence	2	$\frac{1}{\sqrt{2}}\lvert\pi_u^+\alpha\,\pi_u^+\beta\,\pi_g^+\alpha\,\pi_g^+\beta[\pi_u^-\pi_g^-(\alpha\beta-\beta\alpha)]\rvert$
	Rydberg	2	$\frac{1}{\sqrt{2}}\lvert\pi_u^+\alpha\,\pi_u^+\beta\,\pi_u^-\alpha\,\pi_u^-\beta[\pi_g^+np\pi_u^+(\alpha\beta-\beta\alpha)]\rvert$
$^3\Pi_g$	Valence	1	$\frac{1}{\sqrt{2}}\lvert1\pi_g^+\alpha\,1\pi_g^+\beta[3\sigma_g\,1\pi_g^-(\alpha\beta+\beta\alpha)]\rvert$
	Rydberg	1	$\frac{1}{\sqrt{2}}\lvert3\sigma_g\alpha\,3\sigma_g\beta[1\pi_g^+\,ns\sigma_g(\alpha\beta+\beta\alpha)]\rvert$
$^1\Pi_g$	Valence	1	$\frac{1}{\sqrt{2}}\lvert1\pi_g^+\alpha\,1\pi_g^+\beta[3\sigma_g\,1\pi_g^-(\alpha\beta-\beta\alpha)]\rvert$
	Rydberg	1	$\frac{1}{\sqrt{2}}\lvert3\sigma_g\alpha\,3\sigma_g\beta[1\pi_g^+\,ns\sigma_g(\alpha\beta-\beta\alpha)]\rvert$
$^3\Pi_u$	Valence	1	$\frac{1}{\sqrt{2}}\lvert1\pi_g^+\,3\sigma_u(\alpha\beta+\beta\alpha)\rvert$
	Rydberg	1	$\frac{1}{\sqrt{2}}\lvert1\pi_g^+\,np\sigma_u(\alpha\beta+\beta\alpha)\rvert$
$^1\Pi_u$	Valence	1	$\frac{1}{\sqrt{2}}\lvert1\pi_g^+\,3\sigma_u(\alpha\beta-\beta\alpha)\rvert$
	Rydberg	1	$\frac{1}{\sqrt{2}}\lvert1\pi_g^+\,np\sigma_u(\alpha\beta-\beta\alpha)\rvert$

[a]The determinantal wave functions use the notation of Ref. 19 for the spatial and spin parts of the one-electron orbitals.

pling expressions of Eq. (5) and diabatic observed values, obtained, e.g., using a coupled-channel analysis of experimental spectra.

The $^{1,3}\Pi_g$ states of O_2 provide another example of an interaction between Rydberg and valence states which differ by two orbitals. Wave functions for the Rydberg state with the configuration $\cdots(3\sigma_g)^2(1\pi_u)^4(1\pi_g)(ns\sigma_g)$ and the valence state with the configuration $\cdots(3\sigma_g)(1\pi_u)^4(1\pi_g)^3$ are given in the second part of Table I. The matrix elements for the electrostatic interactions between these valence and Rydberg states, expressed in terms of the integral

$$M=\int 3\sigma_g(1)1\pi_g^-(1)\frac{e^2}{r_{12}}ns\sigma_g(2)1\pi_g^+(2)d\tau_1\,d\tau_2, \tag{6}$$

are given by

$$H^{\mathrm{el}}(^1\Pi_g)=-H^{\mathrm{el}}(^3\Pi_g)=M. \tag{7}$$

In the case of configurations which differ by only one orbital, it is well known that, if the orbitals are solutions of the self-consistent Hamiltonian, the interaction between the states is exactly zero, corresponding to an interaction between monoexcited configurations (Brillouin's theorem).

This article is copyrighted as indicated in the article. Reuse of AIP content is subject to the terms at: http://scitation.aip.org/termsconditions. Downloaded to IP: 150.203.176.45 On: Fri, 24 Apr 2015 03:26:09

The diabatic, or crossing, potentials must be defined in a lower-order approximation, assuming that the orbitals are not the self-consistent orbitals. The interaction matrix element is then nonzero. In this approximation, the couplings between the $\cdots(1\pi_u)^4(1\pi_g)(3p\sigma_u)$ Rydberg and $\cdots(1\pi_u)^4(1\pi_g)\times(3\sigma_u)$ valence $^{1,3}\Pi_u$ states obey the relation:

$$H^{\rm el}(^3\Pi_u)=H^{\rm el}(^1\Pi_u)-2M', \tag{8}$$

where

$$M'=\int 1\pi_g^{+}{}^*(1)3\sigma_u(1)\frac{e^2}{r_{12}}np\sigma_u(2)1\pi_g^{+}(2)d\tau_1\,d\tau_2. \tag{9}$$

All quantities in Eq. (8) have the same sign with $|M'|\ll|H^{\rm el}(^{1,3}\Pi_u)|$. The relation expressed in Eq. (8) can be understood by analogy, since, when the σ_u orbitals in Eq. (9) are identical, Eq. (8) represents the energy and it is well known that the energy of the triplet state is lower than that of the singlet state by just twice the exchange integral [see Eq. (3)].

C. Isoconfigurational spin–orbit interactions

Single-configuration estimates of the spin–orbit interaction are generally very good.[19] Using the electronic wave functions of Table I, together with the one-electron microscopic form of the spin–orbit operator $\mathbf{H}^{\rm so}=\Sigma_i\hat{a}_i\mathbf{l}_i\cdot\mathbf{s}_i$, the isoconfigurational spin–orbit interactions can be deduced both for the Rydberg and for the valence states of interest to this work.

For both the $\pi_g np\sigma_u$ Rydberg and $\pi_g 3\sigma_u$ valence states, it follows that[25]

$$\langle^3\Pi_{u1}|\mathbf{H}^{\rm so}|^1\Pi_{u1}\rangle=a_{\pi_g}/2=\langle^3\Pi_{u2}|\mathbf{H}^{\rm so}|^3\Pi_{u2}\rangle=A(^3\Pi_u), \tag{10}$$

where $a_{\pi_g}=\langle\pi_g|\hat{a}|\pi_g\rangle>0$ is a single-electron integral expected to be roughly similar in magnitude to the atomic spin–orbit parameter $\zeta_{\rm O}(2p)=151\ {\rm cm}^{-1}$, and $A(^3\Pi_u)$ is the diagonal spin–orbit constant. Since $A(^3\Pi_u)$ for the Rydberg state is known experimentally ($\approx 95\ {\rm cm}^{-1}$),[18] single-configuration values for a_{π_g}, and all spin–orbit matrix elements expressible in terms of a_{π_g}, may be obtained easily. Similarly, for the $\pi_g ns\sigma_g$ Rydberg and $3\sigma_g\pi_g^3$ valence states,

$$\langle^3\Pi_{g1}|\mathbf{H}^{\rm so}|^1\Pi_{g1}\rangle=a_{\pi_g}/2=\pm A(^3\Pi_g), \tag{11}$$

where the upper sign applies to the Rydberg state, the lower to the inverted valence state.

For the $\pi_g np\pi_u$ Rydberg states, we have

$$\langle^3\Sigma_{u1}^-|\mathbf{H}^{\rm so}|^3\Sigma_{u1}^+\rangle=(a_{\pi_g}-a_{np\pi_u})/2\approx a_{\pi_g}/2, \tag{12a}$$

$$\langle^3\Delta_{u2}|\mathbf{H}^{\rm so}|^1\Delta_{u2}\rangle=(a_{\pi_g}-a_{np\pi_u})/2\approx a_{\pi_g}/2, \tag{12b}$$

$$\langle^3\Sigma_{u0}^{\pm}|\mathbf{H}^{\rm so}|^1\Sigma_{u0}^{\mp}\rangle=(a_{\pi_g}+a_{np\pi_u})/2\approx a_{\pi_g}/2, \tag{12c}$$

$$\langle^3\Delta_{u3}|\mathbf{H}^{\rm so}|^3\Delta_{u3}\rangle=(a_{\pi_g}+a_{np\pi_u})/2=2A(^3\Delta_u)\approx a_{\pi_g}/2. \tag{12d}$$

Since the operator $\mathbf{H}^{\rm so}$ varies as $1/r_k^3$, where r_k represents the distance from an electron to the kth nucleus, $a_{np\pi_u}$ for the diffuse Rydberg orbital is relatively small compared with a_{π_g}, leading to the final approximations in Eq. (12). Similar expressions have been given in Ref. 26.

For the $\pi_u^3\pi_g^3$ valence states, it follows that

$$\langle^3\Sigma_{u1}^-|\mathbf{H}^{\rm so}|^3\Sigma_{u1}^+\rangle=(a_{\pi_g}-a_{\pi_u})/2\approx 0, \tag{13a}$$

$$\langle^3\Delta_{u2}|\mathbf{H}^{\rm so}|^1\Delta_{u2}\rangle=(a_{\pi_g}-a_{\pi_u})/2\approx 0, \tag{13b}$$

$$\langle^3\Sigma_{u0}^{\pm}|\mathbf{H}^{\rm so}|^1\Sigma_{u0}^{\mp}\rangle=-(a_{\pi_g}+a_{\pi_u})/2\approx -a_{\pi_g}, \tag{13c}$$

$$\langle^3\Delta_{u3}|\mathbf{H}^{\rm so}|^3\Delta_{u3}\rangle=-(a_{\pi_g}+a_{\pi_u})/2=2A(^3\Delta_u)\approx -a_{\pi_g}. \tag{13d}$$

For homonuclear molecules, if the molecular π orbitals are expressed as linear combinations of atomic orbitals centered on each nucleus, and the atomic overlap integral is neglected, then $a_{\pi_u}\approx a_{\pi_g}$,[19] leading to the final approximations in Eq. (13).

Finally, we note that spin–orbit interactions between the valence and Rydberg states of interest here are zero in the single-configuration approximation.

III. SEMIEMPIRICAL ANALYSIS OF EXPERIMENT

The perturbations, predissociations, and other observable effects resulting from interactions between the Rydberg and valence states depicted in Fig. 1 enable the experimental characterization of those interactions for comparison with the expressions derived in Sec. II B. In this section, we summarize a comprehensive study of Rydberg-valence interactions in O_2 which uses the coupled-channel Schrödinger equations (CSE) method[27,28] to analyze available experimental data. Detailed aspects of this study have been,[11,17,18] or will be, reported elsewhere.

Reliable CSE analyses require access to a wide range of experimental data, covering as large an energy range as possible. In the case of the $^{1,3}\Pi_g$ states, $(2+1)$-photon resonance-enhanced multiphoton-ionization (REMPI) spectra involving excitation from the $X\ ^3\Sigma_g^-$ and $a\ ^1\Delta_g$ states were employed,[14,29,30] together with kinetic energy-release spectra,[10,31] as detailed in Ref. 11. For the $^3\Pi_u$ states, single-photon spectra for absorption from the X state, measured in this[18] and other[32] laboratories, were used, together with fluorescence-excitation spectra,[33,34] in the manner described in Ref. 18. For the $^3\Sigma_u^{\pm}$ and $^1\Sigma_u^+$, states, partially analyzed in Ref. 17, X-state photoabsorption spectra measured in this laboratory were employed,[17,35–38] supplemented by spectrographic data involving excitation from the $X\ ^3\Sigma_g^-$ and $b\ ^1\Sigma_g^+$ states,[39,40] and fluorescence-excitation spectra.[33,34] In the case of the $^1\Pi_u$ and $^{1,3}\Delta_u$ states, the prime sources of data were a-state photoabsorption spectra measured in this[41] and other[42] laboratories, together with spectrographic data.[43] The principal quantities reduced from these spectra for comparison with the CSE calculations were vibronic energies, rotational constants, predissociation linewidths, vibronic intensities, and absolute continuum photoabsorption cross sections.

The CSE formalism employed here has been described in detail in Ref. 17. Briefly, the interacting excited states were described in a diabatic basis and the coupled-channel

This article is copyrighted as indicated in the article. Reuse of AIP content is subject to the terms at: http://scitation.aip.org/termsconditions. Downloaded to IP: 150.203.176.45 On: Fri, 24 Apr 2015 03:26:09

radial wave function obtained by solving the corresponding coupled equations was used, together with an initial-state vibrational wave function and diabatic electronic transition moments, to calculate the photodissociation cross section appropriate for comparison with the experimental data, either directly, or through derived parameters. For all symmetries considered, at least two Rydberg states ($n=3$ and 4) were included in the diabatic basis, as were the important Rydberg-valence and spin–orbit interactions discussed in Secs. II B and II C, respectively. These off-diagonal elements were assumed to be independent of the internuclear distance R. Initial Rydberg potential-energy curves were taken to have shapes similar to that of the ionic $X\,^2\Pi_g$ curve, appropriately displaced in energy, while *ab initio* calculations[44] and experimentally based Rydberg–Klein–Rees curves were employed for the initial valence potentials. In an iterative least-squares-fitting procedure, the CSE model parameters were adjusted[45] so as to optimize agreement with experiment. The particular model parameters of interest here are the optimized Rydberg potential-energy curves, together with the optimized Rydberg-valence and spin–orbit couplings. These deperturbed diabatic parameters are appropriate for comparison with the expressions derived in Sec. II.

Results of the CSE analyses are illustrated in Fig. 2 for two extreme cases of Rydberg-valence mixing. In Fig. 2(a), final potential-energy curves are shown for the $^3\Sigma_u^+$ states. In this case, the Rydberg-valence mixing is small ($|H^{\rm el}|=420$ cm^{-1}) and a diabatic picture is appropriate, observed energy levels of the $D\,^3\Sigma_u^+$ and $G\,^3\Sigma_u^+$ states being most closely associated with the pure $3p\pi_u$ and $4p\pi_u$ Rydberg potentials, respectively. Spin–orbit interaction between the $np\pi_u\,^3\Sigma_{u1}^+$ and $^3\Sigma_{u1}^-$ Rydberg states ($H^{\rm so}=95$ cm^{-1}) plays an important role, providing a perturbation mechanism additional to Rydberg-valence mixing, and, through $^3\Sigma_u^-$ Rydberg-valence mixing, a competing indirect predissociation channel. In addition, in spectra involving excitation from the $X\,^3\Sigma_g^-$ state, the same spin–orbit interaction provides the mechanism for the borrowing of intensity from allowed transitions into the $^3\Sigma_u^-$ states, leading to ready observation of the forbidden $^3\Sigma_u^+\leftarrow X\,^3\Sigma_g^-$ transitions. In Fig. 2(b), final potential-energy curves are shown for the $^1\Pi_u$ states. In this case, the Rydberg-valence mixing is very large ($|H^{\rm el}|=6700$ cm^{-1}) and the adiabatic potentials (dashed lines) differ markedly from the diabatic potentials (solid lines). An adiabatic picture is appropriate here, with the observed levels of the $g\,^1\Pi_u$ and $h\,^1\Pi_u$ states being most closely associated with the bound portion of the lower adiabatic curve, and the double-minimum upper adiabatic curve, respectively. A similar situation applies to the isoconfigurational $^3\Pi_u$ states, but, since the Rydberg-valence crossing point for the triplet lies at a smaller R value than that for the singlet [see Fig. 1(c)], in this case, the lower adiabatic potential has a shoulder, rather than a bound portion, and the outer minimum of the upper double-minimum $F\,^3\Pi_u$ adiabatic potential is deeper than the inner minimum (see Fig. 3 of Ref. 18), in contrast to the case for the $h\,^1\Pi_u$ state. Spin–orbit interaction between the $np\sigma_u\,^1\Pi_{u1}$ and $^3\Pi_{u1}$ Rydberg states ($H^{\rm so}=95$ cm^{-1}) also produces easily observable effects, most noticeably unequal triplet splittings through perturbation of the $^3\Pi_{u1}$ component, and also the appearance of some transitions to the $^1\Pi_u$ state in ground-state spectra,[46] through intensity borrowing from the $^3\Pi_u\leftarrow X\,^3\Sigma_g^-$ transitions.

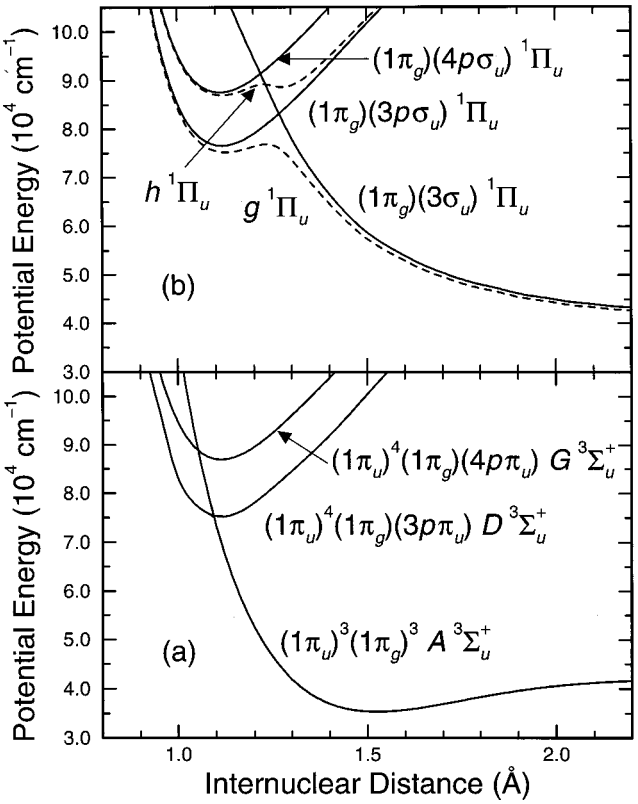

FIG. 2. Diabatic (solid lines) and adiabatic (dashed lines) potential-energy curves resulting from coupled-channel analyses of experiment for two extreme cases of Rydberg-valence interaction in O_2. The energy scale is referenced to the minimum in the $X\,^3\Sigma_g^-$ potential-energy curve. (a) The $^3\Sigma_u^+$ states. In this case, the interaction is small ($|H^{\rm el}|=420$ cm^{-1} for $n=3$), the diabatic and adiabatic curves are indistinguishable on the scale of the figure, and a *diabatic* picture is appropriate. Observed vibrational levels of the $D\,^3\Sigma_u^+$ and $G\,^3\Sigma_u^+$ states can be associated with the diabatic $3p\pi_u$ and $4p\pi_u$ Rydberg potentials, respectively. (b) The $^1\Pi_u$ states. In this case, the interaction is large ($|H^{\rm el}|=6700$ cm^{-1} for $n=3$), the diabatic and adiabatic curves differ greatly, and an *adiabatic* picture is appropriate. Observed vibrational levels of the $g\,^1\Pi_u$ and $h\,^1\Pi_u$ states can be associated with the bound portion of the lower adiabatic potential, and the double-minimum upper adiabatic potential, respectively.

IV. RESULTS AND DISCUSSION

A. Rydberg energies, Rydberg-valence and spin–orbit interactions

Observed diabatic energies for states from the $np\pi_u$, $ns\sigma_g$, and $np\sigma_u$ Rydberg series converging on the ground state of O_2^+, determined using the CSE analysis of experiment described in Sec. III, are summarized for $n=3$ and 4 in Table II, together with corresponding quantum defects δ and effective quantum numbers $n^*=n-\delta$ obtained using the Rydberg formula:

$$E_n=E_\infty-\frac{\mathcal{R}}{(n^*)^2}, \tag{14}$$

This article is copyrighted as indicated in the article. Reuse of AIP content is subject to the terms at: http://scitation.aip.org/termsconditions. Downloaded to IP: 150.203.176.45 On: Fri, 24 Apr 2015 03:26:09

TABLE II. Diabatic energies, effective quantum numbers, and quantum defects for states from the $np\pi_u$, $ns\sigma_g$, and $np\sigma_u$ Rydberg series of O_2 converging on the $X\ ^2\Pi_g$ state of O_2^+.[a]

		$n=3$					$n=4$				
Ryd. Orb.	Symm.	T_e(obs.)[b]	T_e(SC)[c]	T_e(IVO)[d]	n^*(obs.)	δ(obs.)	T_e(obs.)[b]	T_e(SC)[e]	T_e(IVO)[d]	n^*(obs.)	δ(obs.)
$np\pi_u$	$^1\Sigma_u^-$		74 280	74 530				86 630	87 110		
	$^3\Delta_u$	74 770(10)	74 770	75 170	2.208	0.792	86 790(20)	86 790	87 270	3.234	0.766
	$^3\Sigma_u^+$	75 260(20)	75 260	75 740	2.232	0.768	86 970(30)	86 950	87 430	3.262	0.738
	$^3\Sigma_u^-$	74 820(50)	74 790	75 980	2.210	0.790	86 880(40)	86 800	87 350	3.248	0.752
	$^1\Delta_u$	75 420(20)	75 450	76 780	2.240	0.760	87 030(30)	87 010	87 830	3.271	0.729
	$^1\Sigma_u^+$	76 130(10)	76 100	77 510	2.278	0.722	87 210(20)	87 220	87 990	3.300	0.700
$ns\sigma_g$	$^3\Pi_g$	65 550(20)		66 220	1.860	1.140	83 290(20)		83 640[f]	2.800	1.200
	$^1\Pi_g$	66 190(20)		67 110	1.879	1.121	83 340(20)		83 800[f]	2.805	1.195
$np\sigma_u$	$^3\Pi_u$	76 060(50)			2.274	0.726	87 170(30)			3.294	0.706
	$^1\Pi_u$	76 470(50)			2.296	0.704	87 500(30)			3.349	0.651

[a]Energies, in cm^{-1}, are T_e values referenced to the minimum of the $X\ ^3\Sigma_g^-$ potential-energy curve.
[b]Diabatic, deperturbed energies from present CSE analysis of experiment (see Sec. III), with uncertainties in parentheses.
[c]From single-configuration (SC) expressions, Eq. (1), with $K^{(0)}=339\ cm^{-1}$, $J^{(2)}=573\ cm^{-1}$, $K^{(2)}=83\ cm^{-1}$, relative to the experimental $^3\Delta_u$ energy.
[d]*Ab initio* IVO calculations of Cartwright *et al.* (Ref. 52), corrected to give T_e values.
[e]From Eq. (1) with $K^{(0)}=108\ cm^{-1}$, $J^{(2)}=183\ cm^{-1}$, $K^{(2)}=27\ cm^{-1}$, i.e., the $n=3$ values scaled by $(n^*)^{-3}$, relative to the experimental $^3\Delta_u$ energy.
[f]Level labeled $3d\sigma_g$ in Ref. 52.

with $\mathcal{R}=109\,735.5\ cm^{-1}$ and $E_\infty=97\,284\ cm^{-1}$.[47] We emphasize that these observed quantities are deperturbed, i.e., the effects of both Rydberg-valence and spin–orbit interactions have been removed.

Quantum defects for the $3p$ states in Table II lie in the range 0.6–0.8 and are systematically smaller by $\sim 4\%$ for $n=4$. Similar behavior has been observed for the np states of other molecules.[48–50] Quantum defects for the $3s\sigma_g$ states are ~ 1.1, consistent with expectation, but those for $n=4$ are larger by $\sim 6\%$. This increase in the quantum defect is accompanied by a rapid decrease in the singlet–triplet splitting from $\sim 640\ cm^{-1}$ for $n=3$, to $\sim 50\ cm^{-1}$ for $n=4$. These effects are discussed in more detail in Ref. 11, and may be attributed to the onset of strong $ns\sigma_g-(n-1)d\sigma_g$ interactions for $n\geqslant 4$ which are absent for $n=3$.[11,51]

The deperturbed energies may be appropriately compared with the results of single-configuration calculations, such as the IVO calculations of Cartwright *et al.*[52] which are also shown in Table II for the $np\pi_u$ and $ns\sigma_g$ states.[53] Fair agreement is found between the observed and calculated energies: the IVO values exceed the observed values by 400–1400 cm^{-1} for $n=3$, and by 400–800 cm^{-1} for $n=4$. However, the calculated separations between the $^1\Sigma_u^+$ and $^3\Delta_u$ states derived from the $np\pi_u$ Rydberg orbitals exceed the observed separations by approximately a factor of 2. In this respect, the preliminary configuration-mixing (CM) calculations of Buenker and Peyerimhoff,[54] which indicate that the $3p\pi_u$ states span a range of $\sim 1600\ cm^{-1}$, are in much better agreement with the observations. However, neither the CM,[54] nor the IVO[52] calculations predict the correct energy ordering for the $3p\pi_u$ states, in particular, the observed order $T_e(^3\Sigma_u^+)>T_e(^3\Sigma_u^-)$. In addition, both calculations predict $3s\sigma_g\ ^1\Pi_g-^3\Pi_g$ energy separations ($\sim 890\ cm^{-1}$ for IVO,[52] $\sim 810\ cm^{-1}$ for MC[54]) significantly larger than observed ($\sim 640\ cm^{-1}$).

Although the IVO approximation gives a reasonable description of the Rydberg energies, it is insufficient to obtain very precise values. However, our analysis in Sec. II A suggests retaining the single-configuration formalism in order to be able to examine the relations between the energies of the various Rydberg states, while introducing *effective* values for the relevant integrals. Initially, it is of particular interest here to examine the utility of the single-configuration Recknagel[24] expressions [Eq. (1)] in descriptions of the $np\pi_u$ Rydberg energies. The relative $3p\pi_u$ IVO energies of Cartwright *et al.*,[52] where Gaussian orbitals have been used to describe the Rydberg orbitals, are well described using Eq. (1) with the following effective values for the integrals:

$$J^{(2)}=686\ cm^{-1},\ K^{(2)}=40\ cm^{-1},\ K^{(0)}=806\ cm^{-1}. \quad (15)$$

On the other hand, if the observed $3p\pi_u$ diabatic energies in Table II are fitted using Eq. (1), the following effective parameters are found:

$$J^{(2)}=573\ cm^{-1},\ K^{(2)}=83\ cm^{-1},\ K^{(0)}=339\ cm^{-1}. \quad (16)$$

Energies calculated using these parameters in Eq. (1), given in Table II, are seen to reproduce the observed values to within $\pm 30\ cm^{-1}$. If it is assumed that the Recknagel parameters scale with $(n^*)^{-3}$, then, using Eq. (16), the values

$$J^{(2)}=183\ cm^{-1},\ K^{(2)}=27\ cm^{-1},\ K^{(0)}=108\ cm^{-1} \quad (17)$$

are implied for the $4p\pi_u$ states. Energies calculated using these parameters in Eq. (1), also given in Table II, reproduce the observed values to within -10 and $+80\ cm^{-1}$. Such a degree of agreement between the observed energies and those implied by Eq. (1) is encouraging, considering that uncertainties in the observed energies are up to $\sim 50\ cm^{-1}$ for the more heavily deperturbed states. It is evident from Table II that no experimental data are available for the $np\pi_u\ ^1\Sigma_u^-$ states. However, the analytical expressions, Eq. (1), enable energies for these states to be predicted (see Sec. IV B).

This article is copyrighted as indicated in the article. Reuse of AIP content is subject to the terms at: http://scitation.aip.org/termsconditions. Downloaded to IP: 150.203.176.45 On: Fri, 24 Apr 2015 03:26:09

TABLE III. $np\pi_u$, $ns\sigma_g$, and $np\sigma_u$ Rydberg-valence couplings $|H^{el}|$, in cm^{-1}.

		$n=3$			$n=4$		
Ryd. Orb.	Symm.	Obs.[a]	SC[b]	*Ab initio*	Obs.[a]	SC[c]	*Ab initio*
$np\pi_u$	$^1\Sigma_u^-$		1800			1020	
	$^3\Delta_u$	770(50)	900	<320[d]	480(250)	510	
	$^3\Sigma_u^+$	420(40)	0		230(50)	0	
	$^3\Sigma_u^-$	4030(30)	3600	4100[e]	2020(30)	2040	
	$^1\Delta_u$	2640(30)	2700	2700[f]	1500(200)	1530	
	$^1\Sigma_u^+$	1600(100)	1800	1900[g]	840(270)	1020	
$ns\sigma_g$	$^3\Pi_g$	620(50)[h]		830/780[i]	170(70)[h,j]		180/460[i]
	$^1\Pi_g$	630(30)[h]		710/660[i]	170(70)[h,j]		170/480[i]
$np\sigma_u$	$^3\Pi_u$	7180(50)[k]		8400/7600[l]	3620(50)[k]		1840/5200[l]
	$^1\Pi_u$	6630(50)		8300/7000[l]	3570(50)		2000/4800[l]

[a]Diabatic, deperturbed couplings from present CSE analysis of experiment (see Sec. III), with uncertainties in parentheses.
[b]From single-configuration (SC) expressions, Eq. (5), with $M^{(0)}=1800\ cm^{-1}$, $M^{(2)}=900\ cm^{-1}$.
[c]From Eq. (5) with $M^{(0)}=1020\ cm^{-1}$, $M^{(2)}=510\ cm^{-1}$, i.e., the $n=3$ values scaled by $(n^*)^{-3/2}$.
[d]Reference 4; effective value from minimal splitting between adiabatic Rydberg and valence potentials.
[e]Reference 8; value at calculated Rydberg-valence crossing point.
[f]Reference 3; effective value from minimal splitting between adiabatic Rydberg and valence potentials.
[g]References 6 and 9; estimated value at Rydberg-valence crossing point ($R=1.34$ Å).
[h]Given in Ref. 11.
[i]Reference 1; value at calculated Rydberg-valence crossing point. Second value has been corrected by us to the diabatic basis employed here.
[j]Singlet and triplet values held equal in fitting procedure.
[k]From simultaneous fit to $^{1,3}\Pi_{u1}$ states. From fit to $^3\Pi_{u0}$ states, Ref. 18 gives 7110 cm^{-1} and 3540 cm^{-1} for $n=3$ and 4 couplings, respectively.
[l]Reference 3; value at calculated Rydberg-valence crossing point. Second value has been corrected by us to the diabatic basis employed here.

While the effective Recknagel parameters implied by the IVO calculations [Eq. (15)] are in accordance with the expected ordering $K^{(0)}>J^{(2)}>K^{(2)}$ (see Sec. II A), the observed effective parameters [Eq. (16)] do not satisfy the relation $K^{(0)}>J^{(2)}$, but satisfy the more important relations $K^{(0)}>K^{(2)}$ and $J^{(2)}>K^{(2)}$. It is interesting that, in a Recknagel study of the experimental energies for the $\pi_g nd\pi_g$ Rydberg states of O_2, Yokelson *et al.*[55] found the same qualitative relationships between the parameters. For the $3d\pi_g$ states, the following effective parameters were deduced:[55]

$$J^{(2)}=166\ cm^{-1},\ K^{(2)}=48\ cm^{-1},\ K^{(0)}=150\ cm^{-1}, \qquad (18)$$

reasonably similar to the present $4p\pi_u$ parameters [see Eq. (17)].

Observed Rydberg-valence couplings involving the $np\pi_u$, $ns\sigma_g$, and $np\sigma_u$ Rydberg states, determined using the CSE analysis of experiment described in Sec. III, are summarized for $n=3$ and 4 in Table III, together with selected *ab initio* values. The present couplings for the $^3\Delta_u$, $^3\Sigma_u^+$, $^1\Delta_u$, $^1\Sigma_u^+$, and $^1\Pi_u$ states represent the first experimentally based values reported for those symmetries. As illustrated for two extreme cases in Fig. 2, Table III confirms that the magnitudes of the couplings are extremely variable. While the case (2) couplings for the $^{1,3}\Pi_u$ states are the largest, the case (1) couplings vary widely depending on the state symmetry. Overall, there is fairly good agreement between the observed and various *ab initio* couplings, with the observed values generally lower, but it should be emphasized that care needs to be taken with the comparisons. The observed couplings have been obtained using a CSE model which assumes no R dependence and results in values applicable principally in the region of the Rydberg-valence crossing points, which vary from $R_x=1.08$ Å to 1.35 Å for the $n=3$ states considered in this work. Thus, the observed couplings have been compared in Table III with *ab initio* values calculated for appropriate values of R_x, where possible. Furthermore, our diabatic potential-energy curves are somewhat dependent on the underlying assumptions of the CSE model, e.g., that of R-independent coupling, and similar problems arise because of differing theoretical definitions of the diabatic states: Spelsberg and Meyer[8] define the diabatic states as those obtained by diagonalization of the operator $\Sigma_i x_i^2$ in the space spanned by the states, whereas Li *et al.*[1,3] diagonalize the x^2+y^2 quadrupole-moment property. This latter method results in nonzero coupling between the $n=3$ and $n=4$ diabatic Rydberg states. In Table III, we give both the *ab initio* couplings calculated directly by Li *et al.*[1,3] and corresponding modified values which have been corrected by us to the diabatic basis employed here, i.e., a basis requiring zero interaction between the Rydberg states.

From Table III, it can be seen that the observed Rydberg-valence couplings for the np and ns states scale differently with n. For all of the $np\pi_u$ and $np\sigma_u$ states for which it has been possible to determine an $n=4$ coupling, the ratio $H^{el}(n=4)/H^{el}(n=3)$ lies in the range 0.50–0.62, consistent with the $(n^*)^{-3/2}$ scaling rule which predicts a

This article is copyrighted as indicated in the article. Reuse of AIP content is subject to the terms at: http://scitation.aip.org/termsconditions. Downloaded to IP: 150.203.176.45 On: Fri, 24 Apr 2015 03:26:09

ratio of ~ 0.57. However, the observed ratio for the $ns\sigma_g$ states is ~ 0.27. This latter result can be attributed to the effects of the $3d-4s$ interactions invoked above to explain the rapid decrease in the singlet–triplet splitting for these states. While the scaling rule consequently fails in this case, it is interesting to note that the ratio of the observed $^1\Pi_g - ^3\Pi_g$ splittings for $n=4$ and $n=3$ (~ 0.09) remains approximately equal to the *square* of the corresponding ratio of the couplings ($0.27^2 = 0.07$).

Although the Hartree–Fock approximation is not valid for the valence states of interest, the single-configuration expressions [Eq. (5)], based on the leading terms in the configuration-interaction expansions of these states, represent the principal new results obtained in Sec. II and enable an effective-parameter description of the relationships between the magnitudes of the Rydberg-valence couplings for the various states of the $np\pi_u$ complexes. Values calculated using Eq. (5) with the effective parameters $M^{(0)} = 1800$ cm^{-1} and $M^{(2)} = 900$ cm^{-1}, shown in Table III, are seen to provide a very good description of the observed couplings for $n=3$, certainly at the $\pm 400-500$ cm^{-1} level. In addition, values calculated assuming the scaling rule, i.e., with $M^{(0)} = 1020$ cm^{-1} and $M^{(2)} = 510$ cm^{-1}, also shown in Table III, reproduce the observed $n=4$ couplings to within ± 200 cm^{-1}. Just as for the energies discussed above, the analytical expressions for the Rydberg-valence couplings enable predictions to be made for the unobserved $np\pi_u\,^1\Sigma_u^-$ states (see Sec. IV B).

In the case of the $3s\sigma_g$ states, the observed equality between the magnitudes of the couplings for the $^1\Pi_g$ and $^3\Pi_g$ states (see Table III) is consistent with Eq. (7) with an effective $|M| = 630$ cm^{-1}. However, the magnitude of the observed $3p\sigma_u\,^3\Pi_u$ coupling exceeds the corresponding $^1\Pi_u$ value by $\sim 11\%$, inconsistent with Eq. (8) which predicts a larger value for the singlet. This apparent inconsistency can be explained by noting the different Rydberg-valence crossing points for the $^1\Pi_u$ and $^3\Pi_u$ states [see Fig. 1(c)], and postulating that the Rydberg-valence couplings decrease significantly with R. The detailed *ab initio* calculations of Li *et al.*[3] support this view: while, for a given R value, the *ab initio* $n=3$ singlet coupling indeed exceeds the triplet coupling, consistent with Eq. (8), at the relevant Rydberg-valence crossing points the calculated singlet coupling is $\sim 8\%$ *less* than the triplet value, consistent with our observations.[56]

Finally, we note that the off-diagonal spin–orbit interactions between the valence states, described in Sec. II C, have little effect on the spectroscopy of the Rydberg states, so it is not possible in general to determine values for these interactions through analysis of the current experimental data. However, as mentioned in Sec. III, the corresponding interactions among the Rydberg states produce noticeable effects. For the $\pi_g 3p\pi_u$ Rydberg states, we have determined the values, $|\langle {}^3\Delta_{u2}|\mathbf{H}^{\mathrm{so}}|{}^1\Delta_{u2}\rangle| = 96 \pm 6$ cm^{-1}, $|\langle {}^3\Sigma_{u0}^-|\mathbf{H}^{\mathrm{so}}|{}^1\Sigma_{u0}^+\rangle| = 99 \pm 4$ cm^{-1}, and $|\langle {}^3\Sigma_{u1}^-|\mathbf{H}^{\mathrm{so}}|{}^3\Sigma_{u1}^+\rangle| = 92 \pm 11$ cm^{-1}, from CSE analysis of experiment. For the other nonzero Rydberg spin–orbit matrix elements which have not been determined explicitly, values fixed at 95 cm^{-1} were found to provide good descriptions of experiment. In this way, most of the single-configuration expressions in Eqs. (10), (11), and (12) have been verified.

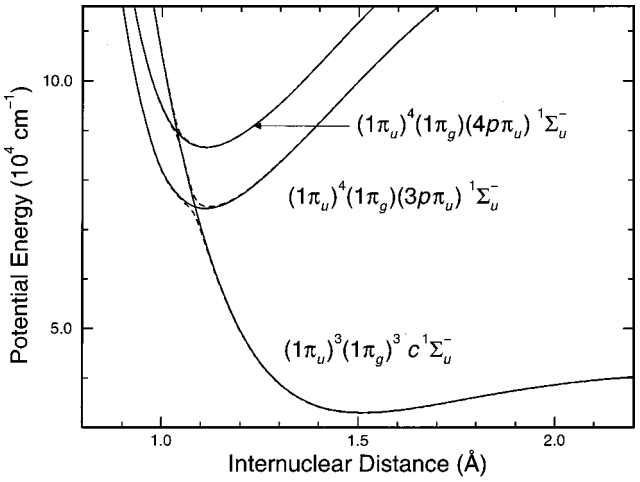

FIG. 3. Diabatic potential-energy curves (solid lines) employed in modeling the $np\pi_u$ Rydberg-valence interactions for the $^1\Sigma_u^-$ states, together with the corresponding adiabatic potentials (dashed lines). The energy scale is referenced to the minimum in the $X\ ^3\Sigma_g^-$ potential-energy curve. In the region of the $n=3$ crossing, the behavior of the $^1\Sigma_u^-$ states is intermediate between diabatic and adiabatic.

B. Predictions for the $^1\Sigma_u^-$ states

Single-photon transitions to the $np\pi_u\,^1\Sigma_u^-$ Rydberg states are electric-dipole-forbidden from the ground $X\ ^3\Sigma_g^-$ and metastable $a\ ^1\Delta_g$ and $b\ ^1\Sigma_g^+$ states of O_2. Furthermore, the first-order intensity-borrowing mechanism which leads to the experimental observation of forbidden transitions such as $3p\pi_u f\ ^1\Sigma_{u0}^+ \leftarrow X\ ^3\Sigma_{g0}^-$ and $3p\pi_u D\ ^3\Sigma_{u1}^+ \leftarrow X\ ^3\Sigma_{g1}^-$, through off-diagonal spin–orbit mixing within the $3p\pi_u$ Rydberg complex [see Eq. (12)], is not available in the case of the $np\pi_u\,^1\Sigma_{u0}^-$ states which are coupled only to the $np\pi_u\,^3\Sigma_{u0}^+$ states [see Eq. (12c)] which are also inaccessible in allowed transitions from the X, a, and b states. Thus, it is not surprising that transitions to the $np\pi_u\,^1\Sigma_u^-$ states have not been observed. However, the analytical expressions, Eqs. (1) and (5), in association with the CSE method summarized in Sec. III, enable some predictions to be made regarding the $^1\Sigma_u^-$ Rydberg-state spectroscopy.

Diabatic potential-energy curves used in the present CSE modeling of the $^1\Sigma_u^-$ Rydberg-valence interaction are shown in Fig. 3 as solid lines. The $c\ ^1\Sigma_u^-$ valence potential was taken from Ref. 57, while the $3p\pi_u$ and $4p\pi_u\,^1\Sigma_u^-$ potentials were taken to have shapes identical to the corresponding $^1\Sigma_u^+$ potentials determined in the study of Sec. III, shifted in energy to have $T_e = 74\,280$ cm^{-1} and $T_e = 86\,630$ cm^{-1}, respectively, as implied by the single-configuration predictions of Table II. The Rydberg-valence interaction matrix elements were taken to be $H^{\mathrm{el}}(n=3) = 1800$ cm^{-1} and $H^{\mathrm{el}}(n=4) = 1020$ cm^{-1}, as implied by the single-configuration predictions of Table III, leading to the adiabatic potential-energy curves shown in Fig. 3 as dashed lines. In the region of the $n=3$ avoided crossing, the adiabaticity parameter[58] $\zeta = H^{\mathrm{el}}(n=3)/\Delta G^{\mathrm{ad}}$, where ΔG^{ad} is the separation of the first vibrational levels of the second adiabatic state, has a

This article is copyrighted as indicated in the article. Reuse of AIP content is subject to the terms at: http://scitation.aip.org/termsconditions. Downloaded to IP: 150.203.176.45 On: Fri, 24 Apr 2015 03:26:09

TABLE IV. Indicative spectroscopic parameters, in cm^{-1}, for the $np\pi_u$ Rydberg-valence coupled $^1\Sigma_u^-$ states of O_2, calculated using the CSE method.

n[a]	v[a]	T_{v0}[b]	B_v	Γ_v[c]
3	0	74 850	1.64	560[d]
3	1	76 250	1.71	600[d]
3	2	78 150	1.64	78
3	3	80 110	1.61	14
3	4	81 960	1.62	180
3	5	83 650	1.64	330
3	6	85 300	1.58	240
4	0	86 860	1.69	33
3	7	87 030	1.54	65
3	8	88 690	1.59	52
4	1	88 810	1.58	10
3	9	90 420	1.52	2
4	2	90 620	1.61	110
3	10	92 120	1.49	20[d]
4	3	92 370	1.63	180[d]

[a]The mixed levels are labeled according to their *predominant* (n,v) character.
[b]Energies are referenced to the virtual level $X\,^3\Sigma_g^-(v=0,\ J=0,\ F_2)$.
[c]FWHM predissociation linewidth.
[d]Approximate value for blended feature.

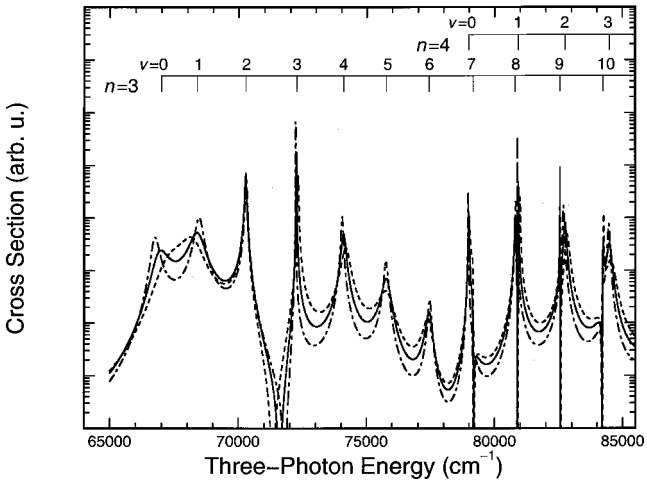

FIG. 4. Indicative rotationless three-photon absorption cross sections for the Rydberg-valence mixed $^1\Sigma_u^- \leftarrow\leftarrow\leftarrow a\,^1\Delta_g(v''=0)$ transitions of O_2, calculated using the CSE method. The solid line: with model parameters of Sec. IV B, including $H^{el}(n=3)=1800\ cm^{-1}$, $H^{el}(n=4)=1020\ cm^{-1}$. The dashed line: with $H^{el}(n=3)=2300\ cm^{-1}$, $H^{el}(n=4)=1300\ cm^{-1}$. The dotted–dashed line: with $H^{el}(n=3)=1300\ cm^{-1}$, $H^{el}(n=4)=735\ cm^{-1}$. The excited-state coupled-channel resonances are labeled according to the (n,v) character of the dominant diabatic Rydberg state.

value of ~ 0.8, implying behavior intermediate between diabatic and adiabatic. Hence, the coupled-channel energy levels will not be strictly associated with either set of potentials. In what follows, however, we will label levels according to their predominant diabatic character. Finally, we note that spin–orbit interactions have not been included in the CSE model employed here, since their inclusion is unlikely to affect the calculated $^1\Sigma_u^-$ energy-level structure significantly, at least at the modest level of uncertainty required for these predictions.

Vibronic energy levels, rotational constants and predissociation linewidths calculated for the Rydberg-valence coupled $^1\Sigma_u^-$ states using this CSE model are summarized in Table IV. Despite conservatively estimated uncertainties of $\sim \pm 100\ cm^{-1}$ in the energy levels and $\sim \pm 50\%$ in the linewidths due to unavoidable uncertainties in the model parameters, several general observations can be made. First, the Rydberg-valence interaction causes strong perturbation and predissociation: the calculated vibrational spacings and rotational constants show erratic variations; in particular, the $n=3$, $v=0$ and 1 levels are abnormally closely spaced and their widths are a significant proportion of that spacing. Second, with the present parameters, the $n=4$, v levels roughly coincide with the $n=3$, $v+7$ levels, leading to the possibility of interesting interference effects. Finally, the degree of predissociation is such that none of the calculated levels is particularly narrow: for $n=3$, there are linewidth minima of 14 cm^{-1} and 2 cm^{-1} full-width at half-maximum (FWHM), at $v=3$ and $v=9$, respectively. This predissociation will, no doubt, significantly hamper the experimental detection of these $^1\Sigma_u^-$ states using normal spectroscopic methods.

Nevertheless, we suggest a possible detection scheme. Transitions from the $a\,^1\Delta_g$ state to $^1\Sigma_u^-$ states are allowed in three-photon absorption, so it may be possible to detect some levels of the $np\pi_u\,^1\Sigma_u^-$ states in $(3+1)$ REMPI experiments involving excitation from this metastable state.[59] In Fig. 4, we show a relative Rydberg-valence coupled $^1\Sigma_u^- \leftarrow\leftarrow \leftarrow a\,^1\Delta_g(v''=0)$ absorption spectrum (the solid line), calculated without rotational structure using the present CSE model with R-independent diabatic three-photon electronic transition moments for $n=3$ and 4.[60] Also shown in Fig. 4 are cross sections calculated for values of the Rydberg-valence couplings at the limits of the estimated uncertainty: $[H^{el}(n=3)=2300\ cm^{-1},\ H^{el}(n=4)=1300\ cm^{-1}$, the dashed line]; $[H^{el}(n=3)=1300\ cm^{-1},\ H^{el}(n=4)=735\ cm^{-1}$, the dotted–dashed line]. While the general observations of the previous paragraph are unchanged with these parameters, it is noticeable from Fig. 4 that, for the highest value of the coupling, transitions into the $n=3$, $v=0$ and 1 levels merge into a single broad predissociating resonance. In REMPI spectra, the detected ion signal suffers from competition between ionization and predissociation,[61] so the narrowest transitions in the absorption spectrum of Fig. 4 will be favored further in the associated REMPI spectrum. Hence, the best possibilities for REMPI detection appear to be the $n=3$, $v=3$ and 9 levels, together with the $n=4$, $v=1$ level.

V. SUMMARY AND CONCLUSIONS

Using a single-configuration formulation, analytical expressions have been derived for the $ns\sigma_g$, $np\pi_u$, and $np\sigma_u$ Rydberg-valence interaction matrix elements in O_2. In particular, new two-parameter expressions have been given for the Rydberg-valence couplings involving the six states arising from the $np\pi_u$ Rydberg orbital. In addition, the results of new, diabatic, coupled-channel deperturbations of experimental data dependent on these interactions have been summarized for $n=3$ and 4. The large differences in magnitude between the Rydberg-valence couplings for the constituent states of the $np\pi_u$ Rydberg complex that are predicted by

This article is copyrighted as indicated in the article. Reuse of AIP content is subject to the terms at: http://scitation.aip.org/termsconditions. Downloaded to IP: 150.203.176.45 On: Fri, 24 Apr 2015 03:26:09

the analytical expressions have been verified experimentally, suggesting that these expressions may be of use in the study of Rydberg-valence interactions in isovalent molecules such as S_2 and SO. Effective values for several two-electron integrals have been obtained semiempirically through comparison between analytical expressions and deperturbed experimental values for the Rydberg-state energies and Rydberg-valence couplings, allowing predictions to be made for the spectroscopy of the $np\pi_u\,{}^1\Sigma_u^-$ Rydberg states which have yet to be observed. An experiment which might allow detection of these states has been suggested.

ACKNOWLEDGMENTS

This paper was prepared during the tenure of H.L.-B. as a Visiting Fellow in the Ultraviolet Physics Unit of the Atomic and Molecular Physics Laboratories at the Australian National University. B.R.L. would like to thank Professor R. J. Buenker for helpful discussions on *ab initio* matrix elements.

[1] Y. Li, I. D. Petsalakis, H.-P. Liebermann, G. Hirsch, and R. J. Buenker, J. Chem. Phys. **106**, 1123 (1997).
[2] Y. Li, M. Honigmann, G. Hirsch, and R. J. Buenker, Chem. Phys. Lett. **212**, 185 (1993).
[3] Y. Li, G. Hirsch, and R. J. Buenker, J. Chem. Phys. **108**, 8123 (1998).
[4] R. J. Buenker and S. D. Peyerimhoff, Chem. Phys. Lett. **34**, 225 (1975).
[5] S. L. Guberman, Planet. Space Sci. **36**, 47 (1987).
[6] S. L. Guberman (private communication).
[7] Y. Li, M. Honigmann, K. Bhanuprakash, G. Hirsch, and R. J. Buenker, J. Chem. Phys. **96**, 8314 (1992).
[8] D. Spelsberg and W. Meyer, J. Chem. Phys. **109**, 9802 (1998).
[9] S. L. Guberman and A. Giusti-Suzor, J. Chem. Phys. **95**, 2602 (1991).
[10] W. J. van der Zande, W. Koot, J. Los, and J. R. Peterson, J. Chem. Phys. **89**, 6758 (1988).
[11] J. S. Morrill, M. L. Ginter, B. R. Lewis, and S. T. Gibson, J. Chem. Phys. **111**, 173 (1999).
[12] W. J. van der Zande, W. Koot, and J. Los, J. Chem. Phys. **91**, 4597 (1989).
[13] R. S. Friedman and A. Dalgarno, J. Chem. Phys. **93**, 2370 (1990).
[14] A. Sur, L. Nguyen, and N. Nikoi, J. Chem. Phys. **96**, 6791 (1992).
[15] J. Wang, D. G. McCoy, A. J. Blake, and L. Torop, J. Quant. Spectrosc. Radiat. Transf. **38**, 19 (1987).
[16] J. Wang, A. J. Blake, D. G. McCoy, and L. Torop, J. Quant. Spectrosc. Radiat. Transf. **40**, 501 (1988).
[17] B. R. Lewis, S. S. Banerjee, and S. T. Gibson, J. Chem. Phys. **102**, 6631 (1995).
[18] J. P. England, B. R. Lewis, S. T. Gibson, and M. L. Ginter, J. Chem. Phys. **104**, 2765 (1996).
[19] H. Lefebvre-Brion and R. W. Field, *Perturbations in the Spectra of Diatomic Molecules* (Academic, Orlando, 1986), pp. 58–59, 208–211, 216–221.
[20] In the principal molecular-orbital notation used here, the filled shells $(1\sigma_g)^2(1\sigma_u)^2(2\sigma_g)^2(2\sigma_u)^2$, common to all states, are suppressed, as is the $(3\sigma_g)^2$ shell where appropriate.
[21] H. Lefebvre-Brion and C. M. Moser, J. Chem. Phys. **43**, 1394 (1965).
[22] H. Lefebvre-Brion, J. Mol. Struct. **19**, 103 (1973).
[23] W. J. Hunt and W. A. Goddard III, Chem. Phys. Lett. **6**, 414 (1969).
[24] A. Recknagel, Z. Phys. **87**, 375 (1934).
[25] Numerical subscripts in the electronic-state designations employed here refer to the value of $|\Omega|$.
[26] R. Ogorzalek-Loo *et al.*, J. Chem. Phys. **91**, 5185 (1989).
[27] E. F. van Dishoeck, M. C. van Hemert, A. C. Allison, and A. Dalgarno, J. Chem. Phys. **81**, 5709 (1984).
[28] L. Torop, D. G. McCoy, A. J. Blake, J. Wang, and T. Scholz, J. Quant. Spectrosc. Radiat. Transf. **38**, 9 (1987).
[29] R. R. Ogorzalek-Loo, Ph.D. thesis, Cornell University, 1989.
[30] A. Sur, R. S. Friedman, and P. J. Miller, J. Chem. Phys. **94**, 1705 (1991).
[31] W. J. van der Zande, W. Koot, J. Los, and J. R. Peterson, Chem. Phys. Lett. **140**, 175 (1987).
[32] K. Ito, K. P. Huber, K. Yoshino, M. Ogawa, and Y. Morioka, J. Mol. Spectrosc. **171**, 1 (1995).
[33] L. C. Lee, T. G. Slanger, G. Black, and R. L. Sharpless, J. Chem. Phys. **67**, 5602 (1977).
[34] S. T. Gibson and B. R. Lewis, J. Electron Spectrosc. Relat. Phenom. **80**, 9 (1996).
[35] B. R. Lewis, S. T. Gibson, M. Emami, and J. H. Carver, J. Quant. Spectrosc. Radiat. Transf. **40**, 1 (1988).
[36] B. R. Lewis, S. T. Gibson, M. Emami, and J. H. Carver, J. Quant. Spectrosc. Radiat. Transf. **40**, 469 (1988).
[37] S. S. Banerjee, Ph.D. thesis, The Australian National University, 1996.
[38] B. R. Lewis *et al.*, J. Chem. Phys. **52**, 2717 (1995).
[39] H. C. Chang, Ph.D. thesis, University of Southern California, 1973.
[40] D. H. Katayama, S. Ogawa, M. Ogawa, and Y. Tanaka, J. Chem. Phys. **67**, 2132 (1977).
[41] P. C. Hill, Ph.D. thesis, The Australian National University, 1991.
[42] S. Ogawa and M. Ogawa, Can. J. Phys. **53**, 1845 (1975).
[43] K. R. Yamawaki, Ph.D. thesis, University of Southern California, 1972.
[44] H. Partridge, C. W. Bauschlicher, Jr., S. R. Langhoff, and P. R. Taylor, J. Chem. Phys. **95**, 8292 (1991); H. Partridge (private communication).
[45] Depending on the quantity and quality of the available experimental data, the significant portions of the Rydberg and valence potential-energy curves were allowed to vary in either a constrained, or an unconstrained, fashion during the fitting procedure.
[46] J. P. England, B. R. Lewis, and M. L. Ginter, J. Chem. Phys. **103**, 1727 (1995).
[47] In Eq. (14), the Rydberg constant $\mathcal{R}$ is mass-corrected and the equilibrium–equilibrium ionization potential from the $X\,{}^3\Sigma_g^-$ state of O_2, E_∞, is averaged over both Ω-components of the $X\,({}^2\Pi_g)$ state of O_2^+.
[48] E. Miescher, J. Mol. Spectrosc. **20**, 130 (1966).
[49] M. Ogawa and S. Ogawa, J. Mol. Spectrosc. **41**, 393 (1972).
[50] M. Eidelsberg and F. Rostas, Astron. Astrophys. **235**, 472 (1990).
[51] S. Chung, C. C. Lin, and E. T. P. Lee, J. Phys. B **21**, 1155 (1988).
[52] D. C. Cartwright, W. J. Hunt, W. Williams, S. Trajmar, and W. A. Goddard III, Phys. Rev. A **8**, 2436 (1973).
[53] Since the IVO calculations (Ref. 52) inherently include the effects of strong Rydberg-valence interactions for the $np\sigma_u$ states, IVO energies for these states are not included for comparison in Table II.
[54] R. J. Buenker and S. D. Peyerimhoff, Chem. Phys. **8**, 324 (1975).
[55] R. J. Yokelson, R. J. Lipert, and W. A. Chupka, J. Chem. Phys. **97**, 6153 (1992).
[56] Note that the *modified* values of Ref. 3, i.e., those corrected to the diabatic basis used here, have been used in drawing this conclusion.
[57] B. Buijsse, W. J. van der Zande, A. T. J. B. Eppink, D. H. Parker, B. R. Lewis, and S. T. Gibson, J. Chem. Phys. **108**, 7229 (1998).
[58] K. Dressler, Ann. Isr. Phys. Soc. **6**, 141 (1983).
[59] A scheme involving three-photon excitation from the $b\,{}^1\Sigma_g^+$ state using a single laser would be unproductive since $\Sigma_u^- \leftarrow\!\leftarrow\!\leftarrow \Sigma_g^+$ transitions are identity-forbidden [D. M. Friedrich, J. Chem. Phys. **75**, 3258 (1981)].
[60] The Rydberg electronic transition moments were assumed to scale with $(n^*)^{-3/2}$ and the valence moment was taken as zero.
[61] B. R. Lewis, S. T. Gibson, J. S. Morrill, and M. L. Ginter, J. Chem. Phys. **111**, 186 (1999).

This article is copyrighted as indicated in the article. Reuse of AIP content is subject to the terms at: http://scitation.aip.org/termsconditions. Downloaded to IP: 150.203.176.45 On: Fri, 24 Apr 2015 03:26:09